Acta Astronautica 144 (2018) 12–22

Contents lists available at ScienceDirect

Acta Astronautica

journal homepage: www.elsevier.com/locate/actaastro

Probability-based hazard avoidance guidance for planetary landing

Xu Yuan [a,b,c], Zhengshi Yu [a,b,c], Pingyuan Cui [a,b,c], Rui Xu [a,b,c,*], Shengying Zhu [a,b,c], Menglong Cao [d], Enjie Luan [e]

[a] *Institute of Deep Space Exploration, Beijing Institute of Technology, Beijing 100081, China*
[b] *Key Laboratory of Autonomous Navigation and Control for Deep Space Exploration, Ministry of Industry and Information Technology, Beijing 100081, China*
[c] *Key Laboratory of Dynamics and Control of Flight Vehicle, Ministry of Education, Beijing 100081, China*
[d] *College of Automation & Electronic Engineering, Qingdao University of Science & Technology, Qingdao 266000, China*
[e] *State Administration of Science, Technology and Industry for National Defense, Beijing 100037, China*

A R T I C L E I N F O

Keywords:
Hazard avoidance
Guidance
Landing
Collision probability
Uncertainty

A B S T R A C T

Future landing and sample return missions on planets and small bodies will seek landing sites with high scientific value, which may be located in hazardous terrains. Autonomous landing in such hazardous terrains and highly uncertain planetary environments is particularly challenging. Onboard hazard avoidance ability is indispensable, and the algorithms must be robust to uncertainties. In this paper, a novel probability-based hazard avoidance guidance method is developed for landing in hazardous terrains on planets or small bodies. By regarding the lander state as probabilistic, the proposed guidance algorithm exploits information on the uncertainty of lander position and calculates the probability of collision with each hazard. The collision probability serves as an accurate safety index, which quantifies the impact of uncertainties on the lander safety. Based on the collision probability evaluation, the state uncertainty of the lander is explicitly taken into account in the derivation of the hazard avoidance guidance law, which contributes to enhancing the robustness to the uncertain dynamics of planetary landing. The proposed probability-based method derives fully analytic expressions and does not require off-line trajectory generation. Therefore, it is appropriate for real-time implementation. The performance of the probability-based guidance law is investigated via a set of simulations, and the effectiveness and robustness under uncertainties are demonstrated.

1. Introduction

Mars and small bodies (asteroids and comets) have always been attracting targets for solar system explorations. Schiaparelli, the Entry, Descent and landing demonstrator Module (EDM) in the first mission of ESA's ExoMars program, has recently attempted a soft landing on Mars. Unfortunately, the Schiaparelli module crashed during its landing attempt on October 19, 2016 due to the saturation of one of the gyroscopes. The second mission of ExoMars is planned for launch in 2020 which comprises a rover and surface science platform [1]. On the other side, based on the success of Curiosity's landing, NASA has announced plans for a new robotic science rover set to launch in 2020 (Mars 2020 Mission) [2], and has set an even more daring goal of sending humans to Mars in the 2030s [3]. China also plans to launch the first Mars probe including an orbiter and a rover around 2020 [4]. As for explorations to small bodies, NASA's NEAR-Shoemaker spacecraft made the first asteroid landing in 2001 [5], and lander Philae of ESA's Rosetta mission made the first comet landing in 2014 [6]. Shortly after Philae's landing, the Japan Aerospace Exploration Agency launched the asteroid sample return spacecraft “Hayabusa 2”, a successor of “Hayabusa” which first in history collected samples from an asteroid and returned to Earth in 2010 [7]. Hayabusa 2 was launched on December 3, 2014, aiming to reach the C-type asteroid 162,173 Ryugu in 2018 and return back to the Earth in 2020 [8]. NASA also launched its first asteroid sampling mission OSIRIS-REx on September 8, 2016, which will travel to the near-Earth asteroid 101,955 Bennu in 2018 and bring a sample back to Earth in 2023 [9]. By exploring the solar system and beyond, scientists are trying to answer key questions such as the origin and evolution of the universe, the solar system and life.

Before landing onto a celestial body, surface characterization and global mapping are usually carried out to establish surface maps for both landing site selection and navigation. However, limited by sensor resolution and environmental perturbations, the surface topography may not be completely characterized with the required accuracy. Hazards like

* Corresponding author. Mail box 22, School of Aerospace Engineering, Beijing Institute of Technology, Beijing 100081, China.
E-mail address: xurui@bit.edu.cn (R. Xu).

https://doi.org/10.1016/j.actaastro.2017.11.039
Received 19 January 2017; Received in revised form 8 September 2017; Accepted 26 November 2017
Available online 9 December 2017

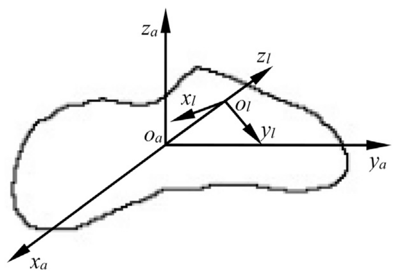

Fig. 1. Celestial-body-fixed and landing-point-fixed coordinate systems.

slopes and boulders hence may not be detected until the lander gets very close to them [10–12]. Particularly, future missions will require pinpoint landing near specific resources which may be situated in potentially hazardous terrains [13–15], and intelligent strategies with active trajectory control are needed to improve mission safety [16]. Therefore, the lander must have onboard hazard avoidance ability to prevent collision and to reach some narrow landing sites.

Representative research on hazard avoidance guidance techniques for planetary landing refers to works by Johnson, A.E., et al. [17], Wong, E.C., et al. [18], de Lafontaine, J., et al. [19], and Rogata, P., et al. [20], in which the polynomial-based guidance algorithms are all adapted from that flown on the Apollo lunar module. A modified polynomial guidance algorithm was developed for the relay hazard avoidance control scheme in China's Chang'e−3 mission that first implemented autonomous hazard avoidance using the onboard measured image data [21,22]. These polynomial-based algorithms are computationally efficient and capable of retargeting to a new landing site, yet unable to include path constraints. These years, interest in spacecraft trajectory optimization has increased [23–25]. In optimization-based methods, the collision avoidance requirements can be explicitly expressed as inequality constraints and fuel expenditure can be minimized [26,27], but most of them are open-loop methods and are sensitive to perturbations. Moreover, the numerical optimization procedure is computationally intensive and unsuitable for real-time implementation. Convex optimization has been paid much attention to, to reduce the computational complexity and guarantee the convergence of the optimization [23,28,29]. A semi-analytical approach has also been proposed, which employs a polynomial form of trajectory and reduces the guidance computation to the optimization of very few parameters [30]. With no optimization involved, the artificial potential function (APF) method is a type of fully analytic closed-loop guidance algorithm that can avoid collision with obstacles or hazards [31,32]. By superimposing an artificial potential field, the negative gradient provides a path that leads the spacecraft away from the obstacles and drives it to the target point. Other guidance algorithms such as the optimal sliding guidance [33] and ZEM/ZEV guidance [34,35], can produce a good approximation of the fuel-optimal trajectory, but collision avoidance function is either not included, or only considered with the altitude constraint to avoid an underground part.

Previous studies of hazard avoidance guidance, as stated above, have different emphases such as low complexity, path constraints inclusion or fuel optimality, but they generally have a deterministic nature, not explicitly taking uncertainty into account. The environment of a planet or small body is very uncertain with different types of perturbations, such as the atmosphere and gusts on a planet, and the irregular gravity field and solar radiation near an asteroid. The accuracy of state estimation is usually limited, and safety state evaluation solely according to the estimated states is sometimes unreliable. Even if designed as a closed-loop system, the hazard avoidance performance may be impacted by large uncertainties. The lander may collide with a hazard even though the estimated position is away from it. Therefore, it is necessary to explicitly take uncertainties into account in the design of guidance method.

This paper investigates a novel probability-based hazard avoidance guidance (PHAG) method for planetary landing, which takes into account the uncertainty of the lander state and generates guidance commands based on the computation of collision probability. The concept of collision probability is introduced, and the collision probability with a hazard is calculated analytically, establishing a probabilistic safety index of the lander instead of simply making use of nominal state information. The collision probability explicitly and accurately quantifies the impact of state uncertainty on the lander safety, and no safety distance or upper bound of uncertainty is used in the design process. This also contributes to avoiding too conservative control effort which may results in excessive fuel consumption and loss of flexibility in trajectory design and landing site selection. Robustness can be enhanced and flexibility of exploration can be preserved, which is advantageous for future advanced missions.

This paper is organized as follows. In Sec. 2, the landing dynamics is formulated and the equations of motion are described. In Sec. 3, the collision probability and its analytic calculation is introduced, and the PHAG law is derived. In Sec. 4, a set of simulation analyses of the proposed PHAG is executed and discussed, to evaluate the effectiveness and robustness of the algorithm under uncertainty. Conclusions drawn are presented in Sec. 5.

2. Equations of motion

In this study, a small body is considered as the central body. For planets, the differences mainly come from the gravity and rotation state, which will be shown later. Two main coordinate systems (c.s.) are considered here: the celestial-body-fixed coordinate system Σ^a, and the landing-point-fixed coordinate system Σ^l .The body-fixed frame Σ^a has its origin at the center of mass of the small body, with the x_a, y_a and z_a axes along the axes of minimum, intermediate, and maximum inertia, respectively. The landing-point-fixed frame Σ^l has its origin O_l at the selected landing site, with the z_l axis along the direction from the center of mass O_a to O_l ($\overrightarrow{O_aO_l}$), y_l axis in the plane of z_a and z_l axes and perpendicular to z_l axis, and the x_l axis satisfies the right-handed rule. An illustrative figure of the two coordinate systems and their relationship is shown in Fig. 1.

It is assumed that the small body spins about the z_a axis with a constant rate ω, and the motion of a lander in the rotating body-fixed frame Σ^a is governed by

$$\ddot{\boldsymbol{r}}_A = \boldsymbol{g} - 2\boldsymbol{\omega} \times \dot{\boldsymbol{r}}_A - \boldsymbol{\omega} \times (\boldsymbol{\omega} \times \boldsymbol{r}_A) + \boldsymbol{a}_{cA} \tag{1}$$

Here, $\boldsymbol{r}_A$ is the spacecraft (S/C) position vector, $\boldsymbol{\omega} = [0, 0, \omega]^{\mathrm{T}}$ is the rotation state vector of the small body, $\boldsymbol{g}$ is the gravitational acceleration, and $\boldsymbol{a}_{cA}$ is the control acceleration exerted on the lander. The subscript A implies these state and control variables are expressed in the body-fixed c.s. The position in body-fixed c.s. is related to the position in landing-point-fixed c.s. by

$$\boldsymbol{r}_A = C_l^a \boldsymbol{r} + \boldsymbol{l} \tag{2}$$

where C_l^a is the transformation matrix from Σ^l to Σ^a, $\boldsymbol{r}$ is the spacecraft position in the landing-point-fixed c.s., and $\boldsymbol{l} = \overrightarrow{O_aO_l}$. Then Eq. (1) becomes

$$C_l^a \ddot{\boldsymbol{r}} = \boldsymbol{g} - 2\boldsymbol{\omega} \times C_l^a \dot{\mathbf{r}} - \boldsymbol{\omega} \times \left[\boldsymbol{\omega} \times \left(C_l^a \boldsymbol{r} + \boldsymbol{l}\right)\right] + C_l^a \boldsymbol{a}_c \tag{3}$$

where $\boldsymbol{a}_c$ is the control acceleration expressed in Σ^l. Multiplying both sides of Eq. (3) by $(C_l^a)^{-1}$, we obtain the equations of motion in the landing-point-fixed c.s. Σ^l

$$\begin{cases} \dot{\boldsymbol{r}} = \boldsymbol{v} \\ \dot{\mathbf{v}} = \boldsymbol{a}_c + \boldsymbol{\xi} \end{cases} \tag{4}$$

where $\boldsymbol{v}$ is the velocity in Σ^l, and

$$\boldsymbol{\xi} = -2\left(C_l^a\right)^{-1}\left(\boldsymbol{\omega} \times C_l^a \boldsymbol{v}\right) - \left(C_l^a\right)^{-1}\left\{\boldsymbol{\omega} \times \left[\boldsymbol{\omega} \times \left(C_l^a \boldsymbol{r} + \boldsymbol{l}\right)\right]\right\} + \left(C_l^a\right)^{-1}\boldsymbol{g} \tag{5}$$